Self-energy and excitonic effects in the electronic and optical properties of TiO_2 crystalline phases

Letizia Chiodo,[1,2] Juan Maria García-Lastra,[1] Amilcare Iacomino,[3,4] Stefano Ossicini,[5] Jin Zhao,[6] Hrvoje Petek,[6] and Angel Rubio[1]

[1]*Nano-Bio Spectroscopy Group and ETSF Scientific Development Centre, Dpto. Física de Materiales, Universidad del País Vasco, Centro de Física de Materiales CSIC-UPV/EHU-MPC and DIPC, Av. Tolosa 72, E-20018 San Sebastián, Spain*

[2]*IIT Italian Institute of Technology, Center for Biomolecular Nanotechnologies, Via Barsanti, Arnesano, I-73010 Lecce, Italy*

[3]*Dipartimento di Fisica "E. Amaldi," Università degli Studi Roma Tre, Via della Vasca Navale 84, I-00146 Roma, Italy*

[4]*CNISM, U. di R. Università degli Studi di Napoli "Federico II," Dipartimento di Scienze Fisiche, Complesso Universitario Monte S. Angelo, Via Cintia, I-80126 Napoli, Italy*

[5]*Dipartimento di Scienze e Metodi dell'Ingegneria, Università di Modena e Reggio Emilia, Via Amendola 2 Pad. Morselli, I-42100 Reggio Emilia, Italy*

[6]*Department of Physics and Astronomy, University of Pittsburgh, Pittsburgh, Pennsylvania 15260, USA*

(Received 27 March 2010; revised manuscript received 23 June 2010; published 22 July 2010)

We present a unified *ab initio* study of electronic and optical properties of TiO_2 rutile and anatase phases with a combination of density-functional theory and many-body perturbation-theory techniques. The consistent treatment of exchange and correlation, with the inclusion of many-body one-particle and two-particles effects in self-energy and electron-hole interaction, produces a high-quality description of electronic and optical properties, giving, for some quantities, the first available estimation for this compound. In particular, we give a quantitative estimate of the electronic and direct optical gaps, clarifying their role with respect to previous measurements obtained by various experimental techniques. We obtain a description for both electronic gap and optical spectra that is consistent with experiments by analyzing the role of different contributions to the experimental optical gap and relating them to the level of theory used in our calculations. We also show the spatial properties of excitons in the two crystalline phases, highlighting the localization character of different optical transitions. This paper aims at understanding and firmly establishing electro-optical bulk properties, yet to be clarified, of this material of fundamental and technological interest for green energy applications.

DOI: 10.1103/PhysRevB.82.045207 PACS number(s): 78.20.Bh, 78.20.Ci, 78.40.−q, 71.35.−y

I. INTRODUCTION

TiO_2 is the paradigm for the electronic, optical, and chemical properties of reducible metal oxides. The response of TiO_2 single-crystal polymorphs, surfaces, and nanostructures to optical excitation is of particular topical interest in solar-energy harvesting through photocatalytic splitting of water into hydrogen and oxygen, in photovoltaic generation of electricity, and reduction in CO_2 into hydrocarbon fuels.[1–3] The photoactive response of TiO_2 nanostructures gained prominence when stable photocatalytic production of H_2 upon band-gap excitation of TiO_2 anatase nanoparticles was demonstrated.[2,4] The interest in solar-energy conversion applications of TiO_2 acquired further impetus through the invention of dye-sensitized solar cells.[1,5,6] Reasons for the continued interest in TiO_2 for solar-energy conversion include the position of its conduction band near the threshold of the energy for hydrogen formation, the relatively long lifetime of conduction-band electrons, the high resistance against corrosion, the high earth abundance, and the low cost.[5,7,8]

In the various technological fields, a fundamental quantity determining the overall behavior of a device is the gap between valence and conduction bands. Depending on the phenomenon, the relevant gap will be the electronic or the optical one. The former one is described by photoemission experiments and connected to a one-particle description. It is related, for instance, to the potentials for the production of H_2 or to the electronic charge injection in solar cells. The optical gap is instead given by light absorption experiments and intrinsically characterized by the copresence of the excited electron and its hole. The fraction of the solar spectrum absorbed is connected to the optical gap, which can be tuned by the combination of TiO_2 with other solid-state materials or organic components.[6,9–15] Whereas the experimental value for the electronic band gap still has a large degree of uncertainty, a general agreement seems to exist in literature concerning the indirect optical-absorption edge of these materials.

As the two types of experiments (photoemission and optical absorption) provide information on two different physical quantities (the former involves a change in the total number of electrons in the material whereas the latter causes the creation of an electron-hole pair with the hole stabilizing the excited electron) the theoretical electronic band gaps obtained by means of density-functional theory (DFT) with local-density approximation/generalized gradient approximation (LDA/GGA),[16,17] hybrid functionals,[18,19] or by many-body calculations[16,17,20,21] should be compared with photoemission data.[20] By contrast, the experimental direct optical band gap should be compared with simulations of the spectra that include excitonic effects [i.e., by using the Bethe-Salpeter equation (BSE) (Refs. 21 and 22)] whereas the indirect optical gap should be compared with models that can take into account higher-order indirect processes involving absorption or emission of phonons. However, incongruous

TABLE I. Calculated electronic gaps from literature obtained with different methods and functionals.

	Method	E_{gap}^{DFT} (eV)	E_{gap}^{GW}	Ref.
Rutile				
	LMTO-ASA+G_0W_0	2.5	4.8, 4.3	20
	LCAO-PBE	1.88		23
	LCAO-PBE0	4.05		23
	PAW-PBE	3.03		23
	PW-PPS-LDA	1.88		26
	QS-GW		3.78	16 and 17
	OLCAO-LDA-AE	1.78		27
Anatase				
	PW-PPs-PBE+G_0W_0	2.05	3.79	28(d)
	LCAO-PBE	2.36 (I)		23
	LCAO-PBE0	4.50 (I)		23
	PAW-PBE	2.08		23
	Gaussian basis, B3LYP	3.7 (4.0 D)		29
	FLAPPW-AE-LDA	2.0 (D)		30
	OLCAO-LDA-AE	2.04 (I)/2.22(D)		27

and confusing comparisons are often made between the theoretical electronic band gap and the experimental indirect optical gap values.[16–19,23–25]

In this introduction we aim to briefly review the results previously obtained using a variety of experimental techniques and *ab initio* calculations in order to elucidate the known properties of bulk TiO_2. Existing computational data (see Table I) will be compared, in the body of the paper, with a complete, consistent *ab initio* description, which includes many-body effects in the calculation of the electronic and optical properties. Most experimental and theoretical data reported from literature refers to the rutile phase (see Fig. 1, top) while anatase (Fig. 1, bottom) in general has been less studied. The anatase polymorph, however, attracts keen interest due in part to its higher photocatalytic activity and greater thermodynamic stability at the nanoscale compared to rutile.[4]

First measurements on the bulk electronic and optical properties of TiO_2 were performed starting from the 1950s (Refs. 32–45) and have been reinvestigated more recently.[46–65] From the photoemission data on rutile[42,44,47,50,53,63] the electronic band gap, corresponding to the difference between the valence-band maximum (VBM) and the conduction-band minimum (CBM), has reported values of 3.3 ± 0.5 eV (Ref. 53) [ultraviolet photoemission spectroscopy (UPS) and inverse photoemission spectroscopy (IPES)], 3.6 ± 0.2 eV (Ref. 63) [UPS and IPES for rutile (110) surface] and ~4.0 eV.[33,50] Assuming that the bulk electronic gap determination is not strongly affected by the surface states, we can adopt a value in the range of 3.3–3.6 eV as a reference for rutile in the following discussion. Keeping also in mind an older measurement of 4.0 eV,[50] quite large degree of uncertainty exists in the experimental electronic gap of the rutile phase. To our knowledge, there are no reported measurements of the electronic band gap for anatase from combined UPS and IPES measurements. An indirect estimation can be obtained from the fact that the electronic direct gap cannot be lower than the direct optical gap, whose value is 3.7–3.9 eV.[64–66]

The experimental results for optical properties of TiO_2 are also of great importance for the photocatalytic and photovoltaic applications of this material. The indirect absorption

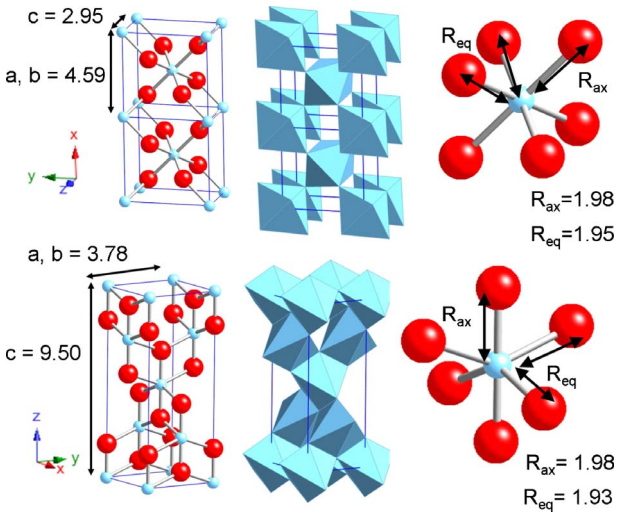

FIG. 1. (Color online) Simple tetragonal unit cell (6 atoms, left), crystallographic structure (center), and TiO_6 octahedrons (right) of rutile (top); and tetragonal conventional cell (12 atoms, left; the unit cell of anatase is a body centered tetragonal with 6 atoms), crystallographic structure (center), and TiO_6 octahedrons (right) of anatase (bottom). Experimental lattice constants and Ti-O distances are indicated in Å. Ti-O distances are larger along the axial direction than in the planar direction of the octahedron. The two phases for rutile and anatase belong to the *P4mmm* and *I4amd* spatial groups, respectively (Ref. 31). The calculated lattice constants in this work are $a=4.65$ Å, $c=2.97$ Å for rutile and $a=3.81$ Å, $c=9.64$ Å for anatase, very close to the experimental values (less than 3% error).

edge, affected by phonon coupling, has been measured to be 3.0 eV (Refs. 34 and 54) for rutile and 3.2 eV (Refs. 25, 52, 55, 67, and 68) for anatase. In rutile the optical edge at 3.03 eV is due to indirect transitions induced by phonon-exciton interactions. The first dipole allowed gap is at 4.2 eV (Ref. 40) and, according to the combined results of absorption, photoluminescence, and Raman-scattering techniques[40] a direct exciton is reported at 3.57 eV.[40,45,69]

The absorption edge of 3.2 eV (Refs. 56 and 57) in anatase is also due to indirect transitions.[55] The first dipole allowed transition energy in anatase can be inferred from optical absorption [3.68 eV (Ref. 66) and 3.80 eV (Ref. 64)] and photoluminescence [below 3.87 eV (Ref. 65)] experiments. Excitons in anatase are found to be self-trapped in the octahedron coordinating the titanium atom, leading to an Urbach tail.[55] This behavior is in contrast to the rutile phase, where the presence of free excitons is ascribed to the packing of octahedra,[55] which is different from the anatase one (see Fig. 1). The influence of the long-range crystalline structure on optical properties will be evident when discussing the spatial distribution of optical excitations in the two phases. Actually the spatial behavior of excitons in TiO_2 has never been investigated but it can be crucial in determining the optical properties of both bulk and nanostructures. Description of excitons, and more in general of optical properties in TiO_2, is complex, because different aspects have to be taken into account. First of all, the ionic character of the compound imparts an important ionic contribution to the screening,[70] which is an order-of-magnitude larger than the pure electronic screening [in rutile, ionic screening values are 111 in the xy plane, 257 along z (Ref. 70)]. Moreover, a strong exciton-phonon interaction has been observed[52,55,70–73] in this compound. The lowest-energy excitonic transitions reported for both phases are indeed due to indirect processes, involving phonon contributions. A further complication arises from the presence of self-trapping phenomena.[52,55,70–73] The exciton creation induces a local ionic relaxation which traps the exciton, localizing it. The copresence of these various effects: polaronic screening,[70] electron-phonon coupling, defects and oxygen vacancies, produces an absorption edge lower in energy than for the direct excitons. Given all these aspects, the nature of excitons, the carrier transport, and the electro-optical role of bulk and surface structure in nanomaterials are still poorly understood.

On the theoretical side (see Table I), due to the intrinsic propensity of DFT to underestimate the electronic band gaps,[74,75] the values obtained at DFT level[16,17,26] are 1.88 eV for rutile (direct at Γ) and 2.05 eV (Ref. 26) (indirect from ~X to Γ) and 2.36 eV (Ref. 23) (direct at Γ) for anatase. When many-body corrections are applied, the resulting electronic gap is around 3.8 eV for both phases.[16,17,28(d)] Either approach, when compared to the optical-absorption edge measured from absorption experiments, clearly gives improper results. The optical gaps (3.0–3.2 eV) are larger than the DFT ones and always smaller than the electronic ones calculated with many-body corrections, due to excitonic effects, phonon-assisted indirect transitions, and temperature effects. When the calculated electronic gap at many-body level is properly compared[20] to photoemission results,[50,53,63] as it is done in the present paper, a quite good agreement can be found.

Some calculations of the optical spectra of these polymorphs[22,30,34,56,59] have been performed at the random-phase approximation (RPA) level, but this description is inappropriate to correctly take into account the optical response of the material, as we show in the results section. By contrast, the many-body description of optics[21,22] gives a substantially improved agreement between the computational spectra and experiments. As discussed in the following, only direct optical transitions contribute to the theoretical description, whereas the phonon-assisted ones are not taken into account. Therefore, a comparison between the direct theoretical and indirect experimental optical edges is inappropriate.

To proceed, the theoretical investigations presented in the literature on the structural, electronic, and optical properties of TiO_2 have been performed sparsely, focusing just on one of the phases, or on some specific property of interest. The use of different methods and levels of theory also makes the results difficult to compare on equal basis. A comprehensive description of properties of both phases in the same theoretical and computational framework is still missing.

We report in this paper a unified *ab initio* description of the optical and the electronic properties treating all the investigated properties at the same level of theoretical framework and complexity. We provide estimation of electronic and direct optical gaps and show the effect of the many-body corrections to the quasiparticle energies on the final absorption spectra and the role of screening anisotropies on the optical response. An important feature is to calculate the optical spectra at a fully *ab initio* level since we used first-principles gap corrections for optics calculations. The very anisotropic spatial distribution of the first allowed optical transitions is related to the crystal structure of the two phases. A comprehensive description of excitons in the two phases is provided through their spectral analysis, their spatial distribution, and the characterization of the electronic states and k points involved in the transitions. These results will be useful when studying the excitonic properties for TiO_2 surfaces,[29,76–86] interfaces and nanostructures,[87–90] and when analyzing the effect of defects and local structural deformations on exciton behavior. This work is organized as follow: we present a short section on the theoretical background, the results for electronic and optical properties, a detailed description of excitons, and finally the conclusions.

II. THEORETICAL METHODS

In this work, state-of-the-art DFT calculations are combined with many-body techniques.[28,91] The structural and energetic description of the rutile and anatase TiO_2 bulk phases have been obtained by DFT,[92,93] a well established tool for the description of ground-state properties. Within DFT we calculate the equilibrium structure, the density of states, and the electronic band structure. *Ab initio* DFT calculations were carried out using the plane-wave code QUANTUM-ESPRESSO.[94] In order to be consistent with the full *ab initio* philosophy of this work, all the results shown here have been obtained using thus calculated geometries. Our

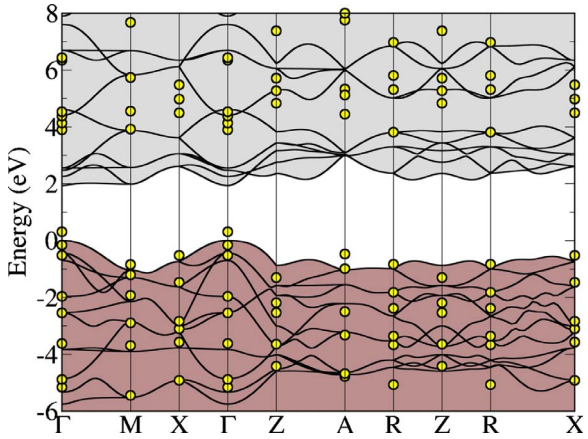

FIG. 2. (Color online) Electronic band structure of rutile bulk along the high symmetry directions of the first Brillouin zone. Black lines indicate the GGA calculation, yellow points indicate the values obtained with the G_0W_0 corrections. The electronic properties have been characterized experimentally by angle-resolved photoemission spectroscopy (Ref. 50) (PES and inverse PES), electrical resistivity (Ref. 33), electroabsorption (Refs. 35 and 36), photoconductivity and photoluminescence (Refs. 37 and 54), x-ray absorption spectroscopy (XAS) (Refs. 38, 39, 41, 43, 46, and 49), resonant Raman spectroscopy (Refs. 48 and 54), photoelectrochemical analysis (Refs. 32 and 67), and electron-energy loss spectroscopy (Refs. 58, 59, and 61). The valence band consists mainly of O $2p$ states partially hybridized with Ti $3d$ states. The metal $3d$ states constitute the conduction band with a small amount of mixing with O $2p$ states. From the symmetry of the TiO_6 octahedra (see Fig. 1), $3d$ states are split by the crystal field into low-energy t_{2g} and high-energy e_g subbands.

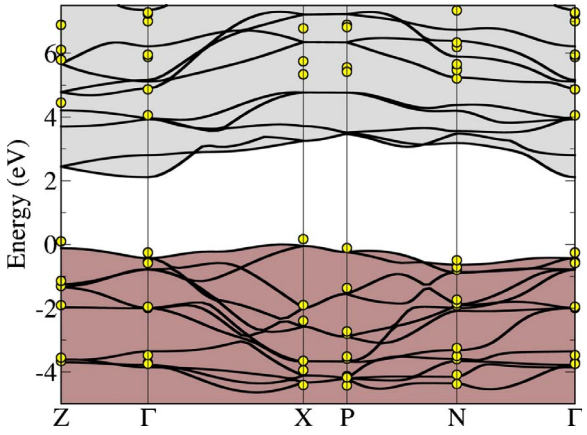

FIG. 3. (Color online) Electronic band structure of anatase bulk along the high symmetry directions of the first Brillouin zone. Black lines indicate the GGA calculation, yellow points indicate the values obtained with the G_0W_0 corrections. Several XAS (Refs. 49, 51, and 52) and photoemission (Refs. 60 and 62) measurements describe electronic structure of anatase, characterizing the p-d hybridization of Ti-O bonds. The valence band of TiO_2 consists mainly of O $2p$ states partially hybridized with Ti $3d$ states. The metal $3d$ states constitute the conduction band with a small amount of mixing with O $2p$ states.

structural and electronic results at DFT level are comparable to data that can be found in literature (see following section).

We apply the standard G_0W_0 calculations to obtain the quasiparticle corrections to the energy levels, starting from the DFT eigenvalues and eigenfunctions,[74,95] as the electronic gap is underestimated in DFT,[74,75] and also the relative positions of s-p-d levels can be affected by this description.

Quasiparticle energies are calculated as corrections to Kohn-Sham eigenvalues, and the proper inclusion of exchange and correlation produces, as shown in the following, an electronic gap in good agreement with experiments. The screening in the G_0W_0 calculation is treated within the plasmon pole approximation. The effect of the so-called local field effects in the screening calculation has been taken into account and carefully converged.

When going from one-electron excited properties, such as the ones described by the electronic levels, to two-particles properties, such as the absorption of light, a further step in the many-body description is necessary, namely, to include the description of the interaction between the excited electron in the conduction band and the hole created in the valence band. As shown in the following, the calculation of the optical absorption spectrum as a sum over transitions of independent particles (RPA),[91] gives in general an incorrect shape and intensity of the peaks, while the inclusion of many-body effects gives the proper optical gap, and a good description of the absorption spectrum and excitons. The inclusion of the excitonic Hamiltonian[91] in the calculation of the optical response provides excitonic eigenvalues and excitonic eigenstates produced by the diagonalization of the excitonic Hamiltonian. The electronic levels are mixed to produce optical transitions, which are not anymore between pairs of independent particles. The resulting eigenvalues describe the excitonic energies, reported in the following. The optical spectra have been obtained at three different theoretical levels: (i) RPA calculations based on the Perdew-Burke-Ernzerhof [(PBE) Ref. 28(a)] energies (RPA@PBE); (ii) RPA calculations based on the G_0W_0 corrected energies (RPA@GW); and (iii) BSE calculations based on the G_0W_0 corrected energies (BSE@GW) and again on the screening obtained at the level (i) driven by the case of the optical spectrum of rutile for the light polarization perpendicular to c direction, screening anisotropy and G_0W_0 effects on the screening were also taken into account at the level (iii) (BSE_2). The reason for this is detailed in the next section. The G_0W_0, optical RPA, and BSE calculations have been performed with the code YAMBO.[96]

III. RESULTS AND DISCUSSION

A. Electronic properties

We calculated for both rutile and anatase, at the DFT level, the band structure (Figs. 2 and 3) along the high symmetry directions, the density of states, and analyzed the spatial behavior of wave functions involved in relevant bonds of the system. We do not report here these results because they are in line with data already published.[20,23,30,50,97] We can say that the comparison with experimental photoemission spectra,[42,44,47,50,53,63] integrated or angular resolved, is quite good, in spite of the well-known difficulties of DFT in describing the d-electron properties.[16,17,98]

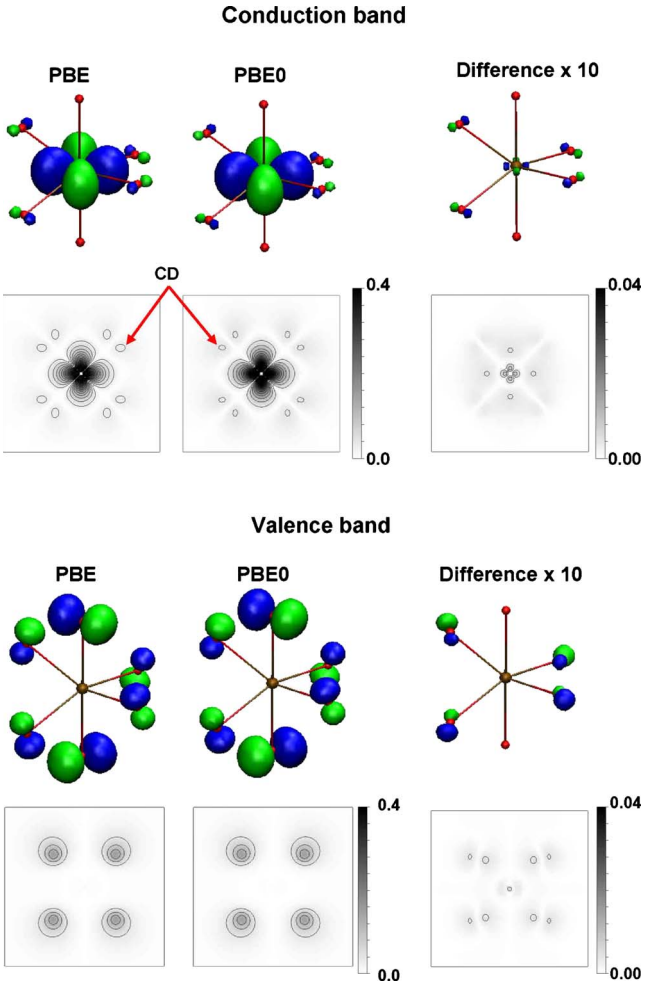

FIG. 4. (Color online) PBE and PBE0 wave functions (and the difference between them) for the valence and conduction bands at Γ point for the anatase phase. Contour plots (absolute values of the wave functions) of the plane $z=0$ are also shown below their corresponding three-dimensional plots. Notice that the scale for the differences is ten times smaller that the one for PBE and PBE0 results. In the case of the valence band the difference in the covalence (labeled CD) is indicated with red arrows.

To take into account the importance of a different wave function starting point for the G_0W_0 calculations onto the electronic description of bulk TiO_2, we compare the spatial localization of Kohn-Sham wave functions obtained from DFT-PBE [Ref. 28(a)] and DFT-PBE0.[28(b),28(c)] In PBE0, the parametrized exchange and correlation contributions are expected to improve the description of electron-localized systems. The results in Fig. 4 indicate that the spatial differences between PBE and PBE0 wave functions are negligible. As it is expected, PBE wave functions show slightly more covalence in the bond between the $2p$ orbitals of the O^{2-} ions and the $3d$ orbitals of the Ti^{4+} ion. This effect is more noticeable in the valence band but in any case the difference in the covalence is below 1% (the valence band has a 14% weight on $2p$ functions of O^{2-} in PBE results and 13% in PBE0 ones). It can be inferred therefore that the election of the functional is not crucial to carry out the G_0W_0 calculations for the defect-free TiO_2 bulk since both wave functions are very similar. Henceforth all the G_0W_0 results shown in this work will have as starting point the PBE wave functions. Our many-body description provides results in quite good agreement with experimental data. As, however, the problem of initial wave functions, and d-electrons localization description, arises for defective systems with oxygen vacancies,[24,99–102] we cannot exclude a major role of exchange-correlation on starting wave functions, and therefore on electronic-optical properties, when defective systems are considered.[19]

The electronic gap, corresponding to the difference between the VBM and the CBM, is calculated (PBE) to be 1.93 eV for rutile (direct gap) and 2.15 eV for anatase (indirect gap), respectively (Table II). The direct gap of anatase is 2.43 eV. The electronic gaps for the two phases are underestimated by almost 1.5–2.0 eV with respect to the (few) experimental data available. Indeed the smallest measured electronic gap for rutile is 3.3 ± 0.5 eV.[53] The application of G_0W_0 to the two systems gives a correction of 1.66 eV and 1.68 eV for rutile and anatase, respectively, calculated at the respective k points of interest. The resulting electronic gaps (direct gap of 3.59 eV for rutile, indirect gap of 3.83 eV, and direct one 4.29 for anatase) are therefore in the range of GW theoretical values (3.7–4.2 eV) reported in literature.[16,17,20,28(d)] The electronic gap for rutile is in good agreement with the experimental estimation given by various techniques, in particular, with the direct estimation (3.3 −3.6 eV) given by the combined photoemission and inverse photoemission experiments.[53,63] The agreement is worse with respect to the value of 4 eV obtained by another photoemission experiment.[50] For anatase, the direct electronic gap is larger than the optical direct edge of 3.7–3.9 eV.[64–66] For both phases, as expected, the electronic gap is definitely larger than the experimental indirect optical gap of 3.0–3.2 eV obtained by, e.g., absorption experiments.[54,55]

In Figs. 2 and 3 the G_0W_0 corrections for high symmetry points of the BZ for rutile and anatase are also reported, plotted as dots on top of the DFT band structure. While the corrections to the valence levels show a linear dependence with the distance from the gap, the corrections to the con-

TABLE II. Calculated electronic band gaps, in electron volt, for rutile and anatase at different levels of theory. Rutile direct gap is at Γ but quite close levels can be found at M and along Γ-M. For anatase indirect and direct electronic gaps are reported. The indirect gap is between a point close to X and Γ, the direct at Γ.

	$PBE_{previous\ works}$	$PBE_{this\ work}$	$GW_{previous\ works}$	$G_0W_{0\ this\ work}$	PES+IPES
Rutile	1.88 (Refs. 23 and 26)	**1.93**	3.78 (Refs. 16 and 17)	**3.59**	3.3,3.6 (Refs. 53 and 63)
Anatase	2.05/2.36 (Refs. 23 and 26)	**2.15/2.43**	3.79 [Ref. 28(d)]	**3.83/4.29**	

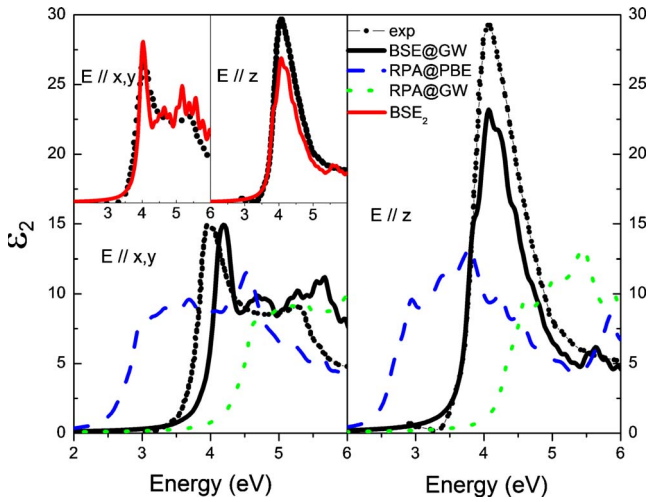

FIG. 5. (Color online) Imaginary part of the dielectric constant for rutile, in-plane polarization *xy* (left) and out-of-plane polarization *z* (right), calculated by GGA random-phase approximation (RPA@PBE, dashed blue line) using G_0W_0 on top of GGA (RPA@GW, dotted light green), and via Bethe-Salpeter equation (BSE@GW, black solid line). The experimental spectrum (solid dotted black, Ref. 34) is also shown for comparison purposes. It is worth to note that experimental absorption spectra with lower intensities of the main peaks (around 13 for *xy* polarization, around 15 for *z* polarization) have been also reported (Ref. 45). Insets: BSE spectrum (BSE_2, red solid line) calculated by including in the screening calculation the proper G_0W_0 electronic gap.

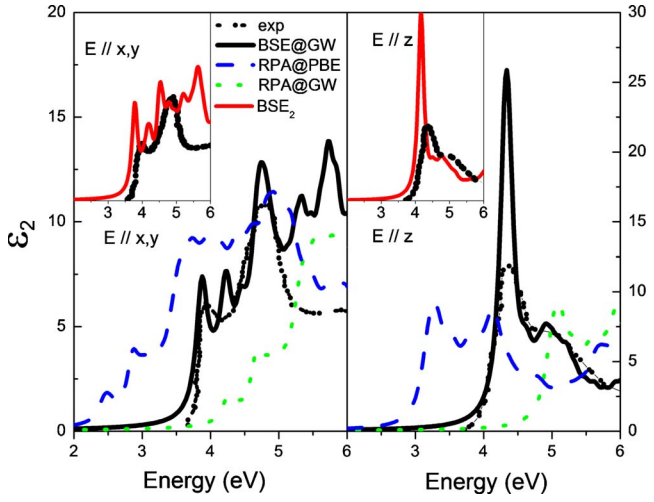

FIG. 6. (Color online) Imaginary part of the dielectric constant for anatase, in-plane polarization *xy* (left) and out-of-plane polarization *z* (right), calculated by GGA random-phase approximation (RPA@PBE, dashed blue line) using G_0W_0 on top of GGA (RPA@GW, dotted light green), and via Bethe-Salpeter equation (BSE@GW, black solid line). The experimental spectrum (solid dotted black, Ref. 34) is also shown for comparison purposes. Insets: BSE spectrum (BSE_2, red solid line) calculated by including in the screening calculation the proper G_0W_0 electronic gap.

duction levels have a more complex behavior, due to the *d* nature of those states. The effect of the nonlinear dependence of the quasiparticle corrections had to be evaluated in the optical spectrum, as discussed in the following paragraph. From Figs. 2 and 3, it is in any case clear that the proper inclusion of correlation through many-body treatment does not change in a dramatic way the relative positions of *d* bands. Even if the use of a rigid scissor operator has to be carefully evaluated for this material, we will show that its use is reasonable in the optical calculations, instead of the full quasiparticle calculation over the first Brillouin zone (IBZ).

B. Optical-absorption properties

It is important to emphasize here that the experimentally determined indirect optical edge does not correspond to the optical band gap given by the first allowed optical transition (with a certain degree of excitonic character). The optical direct transitions are evaluated within the *ab initio* methods used here. In the experimental optical edge, higher-order processes, such as the simultaneous absorption of a photon and scattering with a phonon, can be involved. The ionic screening is also present in experimental data. Moreover, the presence of defects, such as oxygen vacancies, can significantly affect optical properties. Both defects and phonons will be present in any experimental sample of the material at finite temperatures. These observations have to be kept in mind when directly comparing experimental measurements with the theoretical results presented in the following.

The optical-absorption spectra calculated for the two phases, with polarization along the directions *x* (or the equivalent one *y*, in the following also called in plane) and *z* (out of plane, along the *c* axis of the cells) of the unitary cells, are reported in Figs. 5 and 6. The spectra given by independent-particle transitions (RPA@PBE level) present two characteristic features: the band edge is underestimated due to the electronic gap underestimation in DFT, and the overall shape of the spectrum is, for both phases, and both orientations, different from the experiment, in the sense that the oscillator strengths are not correct. The inclusion of the quasiparticle description (RPA@GW), which improves the electronic gap description, does not affect the overall shape of the spectrum, and acts effectively as a scissor operator. We checked that the spectrum shape is almost unchanged, at RPA@GW level, if the two methods (full *ab initio* calculation of G_0W_0 corrections for all the eigenvalues involved in the transitions or *ab initio* calculation of G_0W_0 correction just for the electronic gap) are used (spectra not shown). The absorption edge of RPA@GW is shifted to higher energies, with respect to RPA@PBE, even higher than expected from absorption experiments. The description of optical properties within the two interacting quasiparticles scheme by solving the BSE (BSE@GW) gives indeed a definite improvement of the result over RPA@GW. There is a significant agreement in the spectrum shape with respect to experiments, indicating that both electronic band gap and direct transitions are properly described by many-body methods. The shape of the spectrum is now well described, with a redistribution of transitions at lower energies, with respect to the RPA results. This weight redistribution of oscillator strengths is due to the inclusion of electron-hole interaction in the optical properties. The calculated optical onset is discussed in Sec. III C

TABLE III. Description of optical transitions including excitonic effects. In parenthesis the values with the screening corrected by the G_0W_0 gap. The VBM used in the text corresponds to band no. 24, the CBM to no. 25. The optical indirect gaps are also shown for comparison purposes.

	Energy (eV)	Experimental energy (eV)	k points	Bands
Rutile xy	3.59 (3.55)	3.57 (Refs. 45 and 69) (exciton)	Γ-X, Γ-M	$24\rightarrow25$
	4.24 (4.03)	4.2 (Refs. 54 and 105) (direct optical gap)	R-Z	$24\rightarrow25,29$
Rutile z	3.93. 4.03. 4.06 (3.89, 3.99,4.02)	>3.6 eV (Ref. 69)	all BZ	$24\rightarrow25$–27
	4.27 (4.23)		R-X; Γ	$21\rightarrow25$; $24\rightarrow25$
Anatase xy	3.90, 4.00 (3.80, 3.96)	3.7–3.9 eV (Refs. 64–66) (direct optical gap)	Γ-Z	$23,24\rightarrow25,26$
	4.02, 4.10 (3.99, 4.03)		Γ-Z; Γ	$23,24\rightarrow25,26$
	4.24 (4.17)		Γ-Z	$23,24\rightarrow25,26$
Anatase z	4.35 (4.21)		Γ-Z	$23,24\rightarrow25,26$
	4.40 (4.32)		Γ-Z	$23,24\rightarrow25,26$
Rutile		3.0 (Refs. 34 and 54) indirect gap		
Anatase		3.2 (Refs. 25, 52, 55, 67, and 68) indirect gap		

based on optical transitions evaluated from BSE eigenvalue calculations.

Going into a more detailed discussion, the agreement for spectral shape is in general very good for both polarizations in the case of anatase, as shown in Fig. 6. The optical-absorption edge is well reproduced along both xy and z. In the in-plane xy direction, we obtain the initial sharp peaks whose shape, with respect to the RPA calculation, clearly indicates an excitonic contribution. In the z direction, the initial peak is however too intense with respect to the experimental data. A possible overestimation of excitonic effect for this peak is discussed at the end of this section (see also insets of Fig. 6).

The correspondence between experiment and our calculated spectrum is also quite good in the case of the z polarization for rutile. The absorption shape is quite well reproduced, the sharp edge of the onset of direct transitions is correct, and also the relative intensities are in good agreement with the optical data (but the intensity of the first peak around 4 eV is underestimated and this is not corrected by changing the screening description: see insets of Fig. 5 and the end of the section). The xy polarization in rutile seems to present some more difficulties in the absorption edge determination. Indeed, the overall spectrum shape is quite good due to the exact description of excitonic effects and electron-hole exchange through BSE solution. The whole spectrum seems however to be shifted by about 0.1–0.2 eV to higher energy with respect to experiments.

Much better agreement can be obtained for rutile in-plane polarization if, when calculating the screening used in the BSE, the opening in the gap produced by G_0W_0 corrections is taken into account (see inset of Fig. 5, left, BSE_2). A larger electronic gap makes the screening less efficient. Therefore the electron-hole interaction is less screened and the interacting levels become more bound. The inclusion of the same effect in the absorption along z does not affect the spectrum (see inset of Fig. 5, right) because the description of the screening along the c axis of rutile is already adequate at RPA@PBE level. These differences in the results are related to the large anisotropy in the electronic dielectric constant of rutile (it is 8.427 parallel to c axis and smaller, 6.843, perpendicular to c axis[103]). For anatase, the electronic dielectric constants (5.41 and 5.82 parallel and perpendicular to c axis, respectively) are much more similar,[104] and this results in a comparable description of the BSE optical properties based on the RPA screening. For anatase, the use of the G_0W_0 gap in the BSE screening does not improve the spectra. It moves slightly the edge of the absorption to too low energies and the overall intensities are in worse agreement with experiments (insets of Fig. 6). Both the first excitonic peak in xy and the first very intense peak in z are too much intense in this case.

C. Analysis of excitonic transitions

As the calculated absorption spectra by many-body methods give in general a good agreement with experimental data, one should expect a reasonably good description of excitonic transitions energies. The analysis of energy, k points and wave functions characterizing optical transitions, as obtained by diagonalizing the Bethe-Salpeter Hamiltonian, are described in the following and reported in Table III. We explain the properties of excitons in the rutile and anatase phases, in both real and reciprocal space, and how their localization affects the optical-absorption spectrum. The analysis of the spatial distribution of some excitons in the two phases is reported in Fig. 7, and provides very interesting information, when combined with the exciton binding energy data.

A direct comparison with data extrapolated from experiments, however, cannot be performed, because of the copresence of several physical effects which are visible in experiments and not taken into account in our description. It is interesting to clarify the various contributions present in the

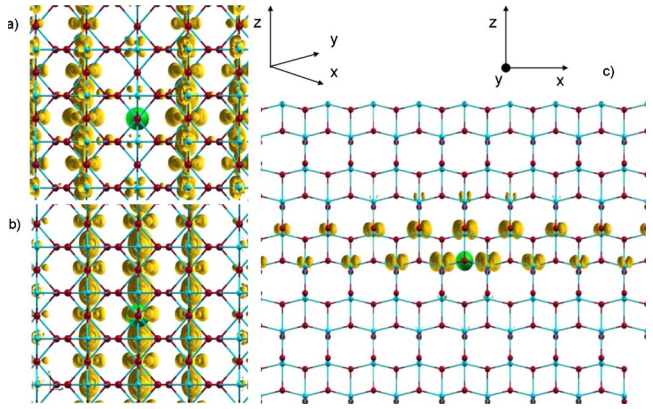

FIG. 7. (Color online) (a) Spatial distribution (yellow isosurfaces in arbitrary units) of the first partial dark exciton at 3.41 eV in rutile for in-plane polarization. The second exciton, at 3.55 eV, is also dark, and shows a spatial wave function similar to the one of the first exciton. (b) Spatial distribution (yellow isosurfaces in arbitrary units) of the third, optically active exciton in rutile, at 3.59 eV, for in-plane polarization. (c) Spatial distribution (yellow isosurfaces in arbitrary units) of the first direct exciton in anatase, at 4.03 eV, in-plane polarization. The hole position in (a)–(c) is denoted by the light green dot, located on an O atom.

experimental absorption spectra of this material, particularly when comparing with theoretical results.

The characteristics of excitons have been debated in this material. The experimental binding energy of the first, indirect exciton in rutile, at 3.03 eV, is reported to be 4 meV.[40,54] Some uncertainty exists in the exact determination of the optical edge. Moreover, excitons are localized in anatase, and delocalized in rutile,[55] at least based on experimental result, but an explanation of this behavior is missing so far.

In TiO_2 polymorphs, direct optical transitions should appear at Γ for rutile and anatase (whose electronic gap is indirect, between Γ and a point close to X). Due to symmetry of *p-d* wave functions, however, these transitions are symmetry forbidden,[70] and the first optical dipole transitions may occur involving other bands than the highest occupied and the lowest empty ones, or different *k* points of the BZ, as shown in the following.

At energies below the direct transition edge, other indirect transitions that occur through mediation by LO and TA phonons have been observed. The electron-phonon interaction is not included in the *ab initio* calculation of the direct transitions. Also the ionic screening, quite large in TiO_2,[70] is not included. The polaron presence can further change the absorption properties because of the local relaxation induced by the exciton creation. The reorganization energy associated with polarons in rutile and anatase is indeed larger than 1 eV, even if structural deformations are small.[71] The excitons described here are not interacting with the system polarized as a whole, but are screened just by the electronic component, and are not interacting with the phonons and the ionic relaxation induced by the exciton creation itself. This explains the differences between our results for optical transition energies and the values reported in literature. Moreover, defects such as oxygen vacancies, very frequent in this oxide, can easily affect the optical spectrum,[106] and defects are not taken into account in our results.

The attribution of the first absorption peak at 3.03 eV for rutile in threshold absorption measurements[40,54] was not clear. It was first supposed to be due to a 1*s* exciton, allowed by a quadrupolar transition, and its binding energy was given as 4 meV. A phonon contribution in this transition was suggested by hyper-Raman-scattering results.[48] Finally the peak was interpreted, in photoluminescence measurements, as a $2p_{xy}$ dipole-allowed phonon-mediated transition,[54,105] for light polarization parallel to *xy*. The experimental direct allowed gap (that is, the first intense structure in the absorption spectrum) is at 4.2 eV.[54,105] In our *ab initio* treatment, processes involving electron-phonon coupling, or quadripolar transitions, are not taken into account. We obtain a good estimation of the intense optical edge in rutile, however. We calculate, for *xy* polarization, the most intense optically allowed transition at 4.24 eV (4.27 eV for *z* polarization), for *k* points belonging to the R-Z direction (R-X for *z* polarization) (see also Fig. 2). The states contributing to these transitions are the VBM and the CBM, and also transitions from VBM to CBM+4 are present. The transition at 4.24 eV corresponds to the first intense peak observed in the absorption spectra. However, we obtain other optical transitions, due to excitons, with oscillator strengths not negligible at energies below 4.24 eV.

The first three excitonic excitations analyzed here are given by transitions from the highest occupied *p* band to the lowest empty *d* band. The first two excitonic transitions [Fig. 7(a)] are optically symmetry forbidden, for in-plane (*xy*) polarization, while the third transitions [Fig. 7(b)] is optically active. It means that, for the first and second transitions, at 3.41 and 3.55 eV, the oscillator strengths have a quite low intensity, as they can be called dark excitons. The BZ point contributing to those transitions is mainly Γ with other points outside of the *xy* plane. The third transition, at 3.59 eV, with larger oscillator strength, is the first bright exciton, and it has contributions from *k* points along Γ-X and Γ-M lines, but it is forbidden at Γ for symmetry reasons. The energetic positions of these first transitions are 3.32, 3.51, and 3.55 eV, when calculated with the screening modified by the G_0W_0 correction of energy levels (see insets of Fig. 5).

As already explained, these excitons are calculated without taking into account the effects of phonons, and therefore, appear at almost 0.4 eV higher energies than the observed forbidden optical gap. Transverse and optical phonons determine the lower optical edge observed in experiments.[40,54,55,69] Direct transitions have been observed[45,69] at 3.57 eV for the in-plane directions, in quite good agreement with our estimation for the first bright exciton (3.59 eV).

With out-of-plane polarization, the first optically allowed transition is at 3.93 eV [the only experimental data to compare with indicates that direct transitions are above 3.6 eV (Ref. 69) for polarization along the *z* direction], followed by other transitions at 4.03 and 4.06 eV. Transitions from the VBM to the CBM, CBM+1, +2 from various high symmetry *k* points distributed in all the BZ contribute to these excitons. The most intense transition is found at 4.27 eV with contributing transitions from *k* points on the R-X direction for the transition VBM-3 to CBM and at Γ from VBM to CBM.

The same transitions, which are symmetry allowed along *z*, are optically forbidden with the in-plane polarization. Cor-

respondingly, all other transitions, apart the ones here listed, are optically dark along the z axis.

The transitions plotted in Figs. 7(a) and 7(b) are from O $2p$ states to Ti $3d$ states of the triply degenerate t_{2g}. While the first two dark exciton transitions involve Ti atoms farther away from the excited O atom, the optically active transition involves states of the nearest-neighbor Ti atoms. The excitons are delocalized in a planar region oriented as the (110) surface. The bright optical exciton is more localized (extending over three lattice constants) in the (110) direction [Fig. 7(b)] with respect to dark excitons. This anisotropic distribution is also related to the anisotropic screening in rutile.

Concerning anatase, the fine structure of the absorption edge has been studied[55] at low temperature. The absorption edge, estimated at 3.2 eV,[34] has a strong phonon contribution, as evident from the existence of an Urbach tail.[107,108] The phenomenon of Urbach tail has received different theoretical explanations,[55] including exciton ionization or exciton self-trapping, both of which require the participation of phonons. In the case of TiO_2, it has been attributed to exciton self-trapping,[55,73,109] i.e., the localization of exciton through phonon coupling. It is favored to occur in anatase with respect to rutile because of the lower coordination between octahedra. The Urbach tail extends to energies below 3.4 eV. Direct optical transitions have been observed, for bulk and thin films, at 3.7–3.9 eV.[64–66]

Our results for anatase show that, with in-plane polarization (xy), the first calculated transition is a direct and the most intense one. It appears at 3.90 eV (3.80 with corrected screening, see insets of Fig. 6) and is given by transitions at the k points along the Γ-Z direction of BZ. The Γ point, however, does not contribute to this exciton, for symmetry reasons. The following allowed transitions at 4.00, 4.02, 4.10, and 4.24 eV (3.96, 3.99, 4.06, and 4.17 eV with corrected screening) are along the Γ-Z direction, and have contributions from the two highest occupied and the two lowest empty bands. The transitions at 4.02 and 4.10 eV also involve contributions from the Γ point. The transitions at 3.90 and 4.24 eV correspond to the first and second sharp peaks observed in the experimental absorption spectra. Along z (out of plane) all the initial transitions allowed in the in-plane directions, are instead dark for symmetry reasons, and the first optically allowed one is at 4.35 eV (4.21 with corrected screening), followed by one at 4.40 eV (4.32 eV). These optical transitions produce the intense peak reported in the spectrum around 4.5 eV. The contributing k points lie along the Γ-Z direction involving the two highest levels of the valence band and the two lowest levels of the conduction band.

The spatial distribution [Fig. 7(c)] shows how the optical excitations, in anatase, have a strong localized character, when compared with rutile. The first exciton is extended for several (at least eight) lattice constants in the xy plane, and, following the chainlike structure of the crystal, is confined in the z direction (it extends along z about for one lattice constant, so it is almost confined to a single atomic plane).

To resume, the direct optical gaps, as estimated from BSE calculations, are in reasonable agreement with experimental data for direct transitions. In rutile we obtain indeed some excitons at energies lower than the direct transition at 4.24 eV, even if their intensities are quite low. In any case, a direct exciton (without interaction with phonons) has been observed, by reflectance, at 3.57 eV (Refs. 45 and 69) with an energy in quite good agreement with our result. If we assume the value of the intense direct optical gap, at 4.24 eV, as reference energy, we obtain a quite large binding energy of 0.65 eV for this low intensity exciton. With respect to the G_0W_0 gap, the exciton binding energy is instead negligible, while the first dark exciton at 3.41 eV is bound by 0.18 eV. For anatase, the optical gap is close but slightly larger than the indirect G_0W_0 gap because it is given by direct transitions along the Γ-Z direction. It turns out to be smaller than the indirect gap when the G_0W_0-corrected screening is used but this is within the uncertainty of these calculations. The effect of electron-hole interaction in anatase is mainly visible in the intensity and in the shape of the spectrum, more than in the exciton binding energy.

Excitons in rutile and anatase have spatial distributions that are determined by the crystal structure and the screening properties of the materials. In both polymorphs, the excitonic wave functions are two dimensional[110] and this planar distribution is localized in just one atomic layer in the anatase case. This stronger localization probably supports the possibility of experimentally reported self-trapping.[55,73,109] The behavior of excitons in anatase have indeed also been modeled within a Franck-Condon model including two-dimensional-exciton transitions.[110] For rutile, the more delocalized distribution of the excitonic wave functions can be connected with the observed[111] low electron-hole recombination rates in this phase.

The finding that excitons are strongly bidimensional in the (001) plane of anatase and almost bidimensional in the (110) plane of rutile, opens interesting scenarios concerning the control of the optical properties of nanostructures with these external surfaces.

IV. CONCLUSIONS

In this paper, we provided a theoretically consistent description of the properties of the two main crystalline phases of titania by means of first-principles calculations based on DFT and GW-BSE. Apart from the advantage of describing, at the same level of theory, different properties of the two systems, we were able to get results in quite good agreement with available photoemission and optical experiments for both rutile and anatase. In particular, we showed that the electronic properties are well described when electron correlations are included in the calculation (at the G_0W_0 self-energy level starting from the GGA wave functions). Moreover, the optical-absorption spectra are quantitatively in good agreement with experiments once electron-hole effects are included even if still some minor discrepancies in the intensities exist for the spectra along different polarization directions. The anisotropy (in particular, in the rutile phase) is shown to be important both in the optical spectra and in the estimation of the screened interaction between hole and electron.

We gave here the first theoretical description of direct excitons in TiO_2 by estimating the first direct optical transition and its exciton binding energy. The excitonic effects act on optical spectra by redistributing the transitions weights, more than by changing the excitonic energies, especially in anatase. The optical excitations are found to be strongly anisotropic. As experimental results suggested, we found a stronger excitonic localization in anatase than in rutile. Excitons have, in both phases, a two-dimensional character, induced by the crystalline structure. In anatase the first bright exciton is completely localized in the (001) plane. In rutile the localization acts in the plane (110). The present characterization of excitonic properties of rutile and anatase will help to understand later on the photophysical response of TiO_2 surfaces, nanowires, and nanoclusters. The excitonic description of pure TiO_2 phases is also the reference starting point for investigation of exciton-phonon interactions, polarons, and defects effects on optical properties of TiO_2 and other titanates. Further work along these lines is now under progress.

Note added in proof. Recently, we became aware of a similar work by Kang and Hybertsen[112] reaching similar conclusions to those of the present work.

ACKNOWLEDGMENTS

We acknowledge funding by "Grupos Consolidados UPV/EHU del Gobierno Vasco" (Grant No. IT-319-07), the European Community through e-I3 ETSF project (Contract No. 211956) and the THEMA-CNT (Contract No. 228539), ACI-Promociona (ACI2009-1036), the Army Research Office under Grant No. W911NF-07-1-0052, National Science Foundation under Grant No. CHE-0650756, and the Spanish Ministerio de Ciencia y Tecnología under Project No. FIS2009-07083. We acknowledge support by the Barcelona Supercomputing Center, "Red Española de Supercomputacion," SGIker ARINA (UPV/EHU), Transnational Access Programme HPC-Europe++, and the supercomputing center of the Environmental Molecular Sciences Laboratory at PNNL, sponsored by the DOE Office of Biological and Environmental Research. L.C. acknowledges funding from UPV/EHU through the "Ayudas de Especialización para Investigadores Doctores" program. H.P. thanks Ikerbasque for the support of his stay at DIPC Donostia International Physics Center. We acknowledge P. Giannozzi, M. Gatti, and M. Palummo for fruitful discussions. A.R. acknowledges fruitful discussions with P. Rinke on many-body correction in oxides and, in particular, on the GW-quasiparticle gap of TiO_2.

[1] A. Fujishima and K. Honda, Nature (London) **238**, 37 (1972).
[2] B. O'Regan and M. Grätzel, Nature (London) **353**, 737 (1991).
[3] V. P. Indrakanti, J. D. Kubicki, and H. H. Schobert, Energy Environ. Sci. **2**, 745 (2009).
[4] A. Fujishima, X. T. Zhang, and D. A. Tryk, Surf. Sci. Rep. **63**, 515 (2008).
[5] M. Grätzel, Nature (London) **414**, 338 (2001).
[6] A. Hagfeldt and M. Grätzel, Acc. Chem. Res. **33**, 269 (2000).
[7] M. R. Hoffmann, S. T. Martin, W. Y. Choi, and D. W. Bahnemann, Chem. Rev. **95**, 69 (1995).
[8] S. U. M. Khan, M. Al-Shahry, and W. B. Ingler, Science **297**, 2243 (2002).
[9] A. Kongkanand, K. Tvrdy, K. Takechi, M. Kuno, and P. V. Kamat, J. Am. Chem. Soc. **130**, 4007 (2008).
[10] Y.-L. Lee, B.-M. Huang, and H.-T. Chien, Chem. Mater. **20**, 6903 (2008).
[11] Y.-Y. Lin, T.-H. Chu, S.-S. Li, C.-H. Chuang, C.-H. Chang, W.-F. Su, C.-P. Chang, M.-W. Chu, and C.-W. Chen, J. Am. Chem. Soc. **131**, 3644 (2009).
[12] O. Niitsoo, S. K. Sarkar, C. Pejoux, S. Rühle, D. Cahen, and G. Hodes, J. Photochem. Photobiol., A **181**, 306 (2006).
[13] R. Plass, S. Pelet, J. Krueger, M. Grätzel, and U. Bach, J. Phys. Chem. B **106**, 7578 (2002).
[14] P. Yu, K. Zhu, A. G. Norman, S. Ferrere, A. J. Frank, and A. J. Nozik, J. Phys. Chem. B **110**, 25451 (2006).
[15] A. Zaban, O. I. Mićić, B. A. Gregg, and A. J. Nozik, Langmuir **14**, 3153 (1998).
[16] M. van Schilfgaarde, T. Kotani, and S. Faleev, Phys. Rev. Lett. **96**, 226402 (2006).
[17] T. Kotani, M. van Schilfgaarde, S. V. Faleev, and A. Chantis, J. Phys.: Condens. Matter **19**, 365236 (2007).
[18] J. Muscat, A. Wander, and N. M. Harrison, Chem. Phys. Lett. **342**, 397 (2001).
[19] A. Janotti, J. B. Varley, P. Rinke, N. Umezawa, G. Kresse, and C. G. Van de Walle, Phys. Rev. B **81**, 085212 (2010).
[20] M. Oshikiri, M. Boero, J. Ye, F. Aryasetiawan, and G. Kido, *Third International Symposium on Transparent Oxide Thin Films for Electronics and Optics (TOEO-3)* (Elsevier Science, Tokyo, Japan, 2003), p. 168.
[21] P. Rinke (private communication).
[22] H. M. Lawler, J. J. Rehr, F. Vila, S. D. Dalosto, E. L. Shirley, and Z. H. Levine, Phys. Rev. B **78**, 205108 (2008).
[23] F. Labat, P. Baranek, C. Domain, C. Minot, and C. Adamo, J. Chem. Phys. **126**, 154703 (2007).
[24] M. V. Ganduglia-Pirovano, A. Hofmann, and J. Sauer, Surf. Sci. Rep. **62**, 219 (2007).
[25] U. Diebold, Surf. Sci. Rep. **48**, 53 (2003).
[26] M. Mikami, S. Nakamura, O. Kitao, H. Arakawa, and X. Gonze, Jpn. J. Appl. Phys., Part 2 **39**, L847 (2000).
[27] S.-D. Mo and W. Y. Ching, Phys. Rev. B **51**, 13023 (1995).
[28] The GGA in the PBE [(a) J. P. Perdew, K. Burke, and M. Ernzerhof, Phys. Rev. Lett. **77**, 3865 (1996)] parametrization for the exchange-correlation potential was employed. Hybrid functional calculations have been performed with PBE0 [(b) C. Adamo and V. Barone, J. Chem. Phys. **110**, 6158 (1999); (c) M. Ernzerhof and G. E. Scuseria, *ibid.* **110**, 5029 (1999)]. Semicore 3*s* and 3*p* states have been included explicitly in the Ti pseudopotential due to their noticeable exchange interaction with the valence states [(d) L. Thulin and J. Guerra, Phys. Rev. B **77**, 195112 (2008)]. Wave function cutoff of 170 Ryd was used to ensure convergence on structural properties. Convergence on energy cutoff has been carefully checked up to 0.01 eV on total energies

and 0.001 eV on eigenvalues using up to 512 k points ($8\times8\times8$ mesh in the Monkhorst-Pack scheme [(e) H. J. Monkhorst and J. D. Pack, *ibid.* **13**, 5188 (1976)] for both phases in the irreducible Brillouin zone (IBZ). K-points meshes of $8\times8\times8$ have been used for both the optical and GW calculations.

[29] A. Beltrán, J. R. Sambrano, M. Calatayud, F. R. Sensato, and J. Andrés, Surf. Sci. **490**, 116 (2001).

[30] R. Asahi, Y. Taga, W. Mannstadt, and A. J. Freeman, Phys. Rev. B **61**, 7459 (2000).

[31] J. K. Burdett, T. Hughbanks, G. J. Miller, J. W. Richardson, and J. V. Smith, J. Am. Chem. Soc. **109**, 3639 (1987).

[32] D. C. Cronemeyer, Phys. Rev. **87**, 876 (1952).

[33] R. G. Breckenridge and W. R. Hosler, Phys. Rev. **91**, 793 (1953).

[34] M. Cardona and G. Harbeke, Phys. Rev. **137**, A1467 (1965).

[35] F. Arntz and Y. Yacoby, Phys. Rev. Lett. **17**, 857 (1966).

[36] A. Frova, P. J. Boddy, and Y. S. Chen, Phys. Rev. **157**, 700 (1967).

[37] A. K. Ghosh, F. G. Wakim, and R. R. Addiss, Phys. Rev. **184**, 979 (1969).

[38] D. W. Fischer, Phys. Rev. B **5**, 4219 (1972).

[39] S. Hüfner and G. K. Wertheim, Phys. Rev. B **7**, 2333 (1973).

[40] J. Pascual, J. Camassel, and H. Mathieu, Phys. Rev. B **18**, 5606 (1978).

[41] L. A. Grunes, Phys. Rev. B **27**, 2111 (1983).

[42] R. G. Egdell, S. Eriksen, and W. R. Flavell, Solid State Commun. **60**, 835 (1986).

[43] F. M. F. de Groot, M. Grioni, J. C. Fuggle, J. Ghijsen, G. A. Sawatzky, and H. Petersen, Phys. Rev. B **40**, 5715 (1989).

[44] R. L. Kurtz, R. Stockbauer, T. E. Madey, E. Roman, and J. L. Desegovia, Surf. Sci. **218**, 178 (1989).

[45] K. Vos, J. Phys. C **10**, 3917 (1977).

[46] G. van der Laan, Phys. Rev. B **41**, 12366 (1990).

[47] R. Heise, R. Courths, and S. Witzel, Solid State Commun. **84**, 599 (1992).

[48] K. Watanabe, K. Inoue, and F. Minami, Phys. Rev. B **46**, 2024 (1992).

[49] F. M. F. de Groot, J. Faber, J. J. M. Michiels, M. T. Czyżyk, M. Abbate, and J. C. Fuggle, Phys. Rev. B **48**, 2074 (1993).

[50] P. J. Hardman, G. N. Raikar, C. A. Muryn, G. Vanderlaan, P. L. Wincott, G. Thornton, D. W. Bullett, and P. Dale, Phys. Rev. B **49**, 7170 (1994).

[51] R. Sanjinés, H. Tang, H. Berger, F. Gozzo, G. Margaritondo, and F. Lévy, J. Appl. Phys. **75**, 2945 (1994).

[52] H. Tang, K. Prasad, R. Sanjines, P. E. Schmid, and F. Levy, J. Appl. Phys. **75**, 2042 (1994).

[53] Y. Tezuka, S. Shin, T. Ishii, T. Ejima, S. Suzuki, and S. Sato, J. Phys. Soc. Jpn. **63**, 347 (1994).

[54] A. Amtout and R. Leonelli, Phys. Rev. B **51**, 6842 (1995).

[55] H. Tang, F. Levy, H. Berger, and P. E. Schmid, Phys. Rev. B **52**, 7771 (1995).

[56] N. Hosaka, T. Sekiya, M. Fujisawa, C. Satoko, and S. Kurita, J. Electron Spectrosc. Relat. Phenom. **78**, 75 (1996).

[57] N. Hosaka, T. Sekiya, C. Satoko, and S. Kurita, J. Phys. Soc. Jpn. **66**, 877 (1997).

[58] M. Arai, S. Kohiki, H. Yoshikawa, S. Fukushima, Y. Waseda, and M. Oku, Phys. Rev. B **65**, 085101 (2002).

[59] N. Vast, L. Reining, V. Olevano, P. Schattschneider, and B. Jouffrey, Phys. Rev. Lett. **88**, 037601 (2002).

[60] A. G. Thomas, W. R. Flavell, A. R. Kumarasinghe, A. K. Mallick, D. Tsoutsou, G. C. Smith, R. Stockbauer, S. Patel, M. Grätzel, and R. Hengerer, Phys. Rev. B **67**, 035110 (2003).

[61] M. Launay, F. Boucher, and P. Moreau, Phys. Rev. B **69**, 035101 (2004).

[62] A. G. Thomas, W. R. Flavell, A. K. Mallick, A. R. Kumarasinghe, D. Tsoutsou, N. Khan, C. Chatwin, S. Rayner, G. C. Smith, R. L. Stockbauer, S. Warren, T. K. Johal, S. Patel, D. Holland, A. Taleb, and F. Wiame, Phys. Rev. B **75**, 035105 (2007).

[63] S. Rangan, S. Katalinic, R. Thorpe, R. A. Bartynski, J. Rochford, and E. Galoppini, J. Phys. Chem. C **114**, 1139 (2010).

[64] Z. Wang, U. Helmersson, and P.-O. Käll, Thin Solid Films **405**, 50 (2002).

[65] B. Liu, L. Wen, and X. Zhao, Mater. Chem. Phys. **106**, 350 (2007).

[66] M. M. Hasan, A. S. M. A. Haseeb, R. Saidur, and H. H. Masjuki, International Journal of Chemical and Biomolecular Engineering **1**, 93 (2008).

[67] L. Kavan, M. Grätzel, S. E. Gilbert, C. Klemenz, and H. J. Scheel, J. Am. Chem. Soc. **118**, 6716 (1996).

[68] H. Tang, H. Berger, P. E. Schmid, F. Lévy, and G. Burri, Solid State Commun. **87**, 847 (1993).

[69] O. Madelung, U. Rössler, and M. E. Schulz, SpringerMaterials—The Landolt-Börnstein Database, http://www.springermaterials.com

[70] C. Persson and A. F. da Silva, Appl. Phys. Lett. **86**, 231912 (2005).

[71] N. A. Deskins and M. Dupuis, Phys. Rev. B **75**, 195212 (2007).

[72] B. J. Morgan and G. W. Watson, Phys. Rev. B **80**, 233102 (2009).

[73] K. Watanabe and T. Hayashi, J. Lumin. **112**, 88 (2005).

[74] R. W. Godby, M. Schlüter, and L. J. Sham, Phys. Rev. B **37**, 10159 (1988).

[75] R. O. Jones and O. Gunnarsson, Rev. Mod. Phys. **61**, 689 (1989).

[76] U. Aschauer, Y. B. He, H. Z. Cheng, S. C. Li, U. Diebold, and A. Selloni, J. Phys. Chem. C **114**, 1278 (2010).

[77] X. Q. Gong, A. Selloni, M. Batzill, and U. Diebold, Nature Mater. **5**, 665 (2006).

[78] X. Q. Gong, A. Selloni, O. Dulub, P. Jacobson, and U. Diebold, J. Am. Chem. Soc. **130**, 370 (2008).

[79] Y. B. He, A. Tilocca, O. Dulub, A. Selloni, and U. Diebold, Nature Mater. **8**, 585 (2009).

[80] M. Lazzeri and A. Selloni, Phys. Rev. Lett. **87**, 266105 (2001).

[81] S. C. Li, J. G. Wang, P. Jacobson, X. Q. Gong, A. Selloni, and U. Diebold, J. Am. Chem. Soc. **131**, 980 (2009).

[82] A. Selloni, Nature Mater. **7**, 613 (2008).

[83] A. Vittadini, M. Casarin, and A. Selloni, Theor. Chem. Acc. **117**, 663 (2007).

[84] A. Vittadini, A. Selloni, F. P. Rotzinger, and M. Grätzel, Phys. Rev. Lett. **81**, 2954 (1998).

[85] O. Bikondoa, C. L. Pang, R. Ithnin, C. A. Muryn, H. Onishi, and G. Thornton, Nature Mater. **5**, 189 (2006).

[86] A. L. Linsebigler, G. Q. Lu, and J. T. Yates, Chem. Rev. **95**, 735 (1995).

[87] R. Buonsanti, V. Grillo, E. Carlino, C. Giannini, M. L. Curri, C. Innocenti, C. Sangregorio, K. Achterhold, F. G. Parak, A. Agostiano, and P. D. Cozzoli, J. Am. Chem. Soc. **128**, 16953 (2006).

[88] A. Iacomino, G. Cantele, D. Ninno, I. Marri, and S. Ossicini, Phys. Rev. B **78**, 075405 (2008).

[89] A. Iacomino, G. Cantele, F. Trani, and D. Ninno, J. Phys. Chem. C (to be published).
[90] A. Petrella, M. Tamborra, M. L. Curri, P. Cosma, M. Striccoli, P. D. Cozzoli, and A. Agostiano, J. Phys. Chem. B **109**, 1554 (2005).
[91] G. Onida, L. Reining, and A. Rubio, Rev. Mod. Phys. **74**, 601 (2002).
[92] P. Hohenberg and W. Kohn, Phys. Rev. **136**, B864 (1964).
[93] W. Kohn and L. J. Sham, Phys. Rev. **140**, A1133 (1965).
[94] P. Giannozzi, S. Baroni, N. Bonini, M. Calandra, R. Car, C. Cavazzoni, D. Ceresoli, G. L. Chiarotti, M. Cococcioni, I. Dabo, A. Dal Corso, S. de Gironcoli, S. Fabris, G. Fratesi, R. Gebauer, U. Gerstmann, C. Gougoussis, A. Kokalj, M. Lazzeri, L. Martin-Samos, N. Marzari, F. Mauri, R. Mazzarello, S. Paolini, A. Pasquarello, L. Paulatto, C. Sbraccia, S. Scandolo, G. Sclauzero, A. P. Seitsonen, A. Smogunov, P. Umari, and R. M. Wentzcovitch, J. Phys.: Condens. Matter **21**, 395502 (2009).
[95] F. Aryasetiawan and O. Gunnarsson, Rep. Prog. Phys. **61**, 237 (1998).
[96] A. Marini, C. Hogan, M. Grüning, and D. Varsano, Comput. Phys. Commun. **180**, 1392 (2009).
[97] K. M. Glassford and J. R. Chelikowsky, Phys. Rev. B **46**, 1284 (1992).
[98] M. Gatti, F. Bruneval, V. Olevano, and L. Reining, Phys. Rev. Lett. **99**, 266402 (2007).
[99] C. Di Valentin, G. Pacchioni, and A. Selloni, Phys. Rev. Lett. **97**, 166803 (2006).
[100] E. Finazzi, C. Di Valentin, G. Pacchioni, and A. Selloni, J. Chem. Phys. **129**, 154113 (2008).
[101] P. Krüger, S. Bourgeois, B. Domenichini, H. Magnan, D. Chandesris, P. Le Fèvre, A. M. Flank, J. Jupille, L. Floreano, A. Cossaro, A. Verdini, and A. Morgante, Phys. Rev. Lett. **100**, 055501 (2008).
[102] T. Minato, Y. Sainoo, Y. Kim, H. S. Kato, K.-i. Aika, M. Kawai, J. Zhao, H. Petek, T. Huang, W. He, B. Wang, Z. Wang, Y. Zhao, J. Yang, and J. G. Hou, J. Chem. Phys. **130**, 124502 (2009).
[103] T. A. Davis and K. Vedam, J. Opt. Soc. Am. **58**, 1446 (1968).
[104] R. J. Gonzalez, R. Zallen, and H. Berger, Phys. Rev. B **55**, 7014 (1997).
[105] A. Amtout and R. Leonelli, Phys. Rev. B **46**, 15550 (1992).
[106] T. Sekiya, S. Kamei, and S. Kurita, J. Lumin. **87-89**, 1140 (2000).
[107] M. Capizzi and A. Frova, Phys. Rev. Lett. **25**, 1298 (1970).
[108] F. Urbach, Phys. Rev. **92**, 1324 (1953).
[109] N. Hosaka, T. Sekiya, and S. Kurita, J. Lumin. **72-74**, 874 (1997).
[110] T. Makino, Y. Segawa, M. Kawasaki, Y. Matsumoto, H. Koinuma, M. Murakami, and R. Takahashi, J. Phys. Soc. Jpn. **72**, 2696 (2003).
[111] R. Katoh, M. Murai, and A. Furube, Chem. Phys. Lett. **461**, 238 (2008).
[112] Wei Kang and M. S. Hybertsen, arXiv:1006.4085 (unpublished).